THE JOURNAL OF PHYSICAL CHEMISTRY B

Article

pubs.acs.org/JPCB

N-Terminal Truncation Does Not Affect the Location of a Conserved Tryptophan in the BLUF Domain of AppA from *Rhodobacter sphaeroides*

Masashi Unno,*[,†] Yuuki Tsukiji,[†] Kensuke Kubota,[†] and Shinji Masuda[‡,§]

[†]Department of Chemistry and Applied Chemistry, Graduate School of Science and Engineering, Saga University, Saga 840-8502, Japan

[§]PRESTO, JST, 4-1-8 Honcho Kawaguchi, Saitama 332-0012, Japan

[‡]Center for Biological Resources and Informatics, Tokyo Institute of Technology, Yokohama 226-8501, Japan

Supporting Information

ABSTRACT: The flavin-binding BLUF domains are a class of blue-light receptors, and AppA is a representative of this family. Although the crystal and solution structures of several BLUF domains have already been obtained, there is a key uncertainty regarding the position of a functionally important tryptophan (Trp104 in AppA). In the first crystal structure of an N-terminally truncated BLUF domain of AppA133 (residues 17−133), Trp104 was found in close proximity to flavin (Trp_{in}), whereas in a subsequent structure with an intact N-terminus AppA126 (residues 1−126), Trp104 was exposed to the solvent (Trp_{out}). A recent study compared spectroscopic properties of AppA126 and AppA133 and claimed that the Trp_{in} conformation is an artifact of N-terminal truncation in AppA133. In this study, we compared the flavin vibrational spectra of AppA126 and AppA133 by using near-infrared excited Raman spectroscopy. In addition, the conformations as well as the environments of Trp104 were directly monitored by ultraviolet resonance Raman spectroscopy. These studies demonstrate that the N-terminal truncation does not induce the conformational switch between Trp_{in} and Trp_{out}.

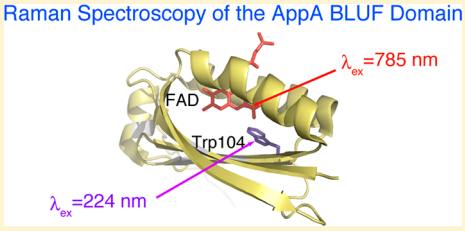

INTRODUCTION

In many biological photoreceptors, such as rhodopsins, phytochromes, photoactive yellow protein, and phototropins, gross structural changes are photoinduced in the chromophore molecule, which triggers a series of protein structural changes that ultimately lead to the formation of a signaling state.[1] In contrast, flavin-containing BLUF (blue-light using flavin adenine dinucleotide (FAD))[2] proteins show a different photoactivation mechanism that is not accompanied by the prominent structural changes of the chromophore.[3,4] In BLUF proteins, the signaling state is characterized by a light-induced ∼10 nm red shift of the UV−visible absorption spectrum[5−12] and ∼16 cm^{-1} downshift of the C4═O stretching mode of the flavin ring.[13−15] These spectroscopic changes are characteristic to BLUF proteins.

Recently, crystal and solution structures of several BLUF domains were obtained.[8,16−22] These structures show that the BLUF domain consists of a five-stranded β-sheet with two α-helices packed on one side of the sheet, with the noncovalently bound isoalloxazine ring of FAD positioned between two α-helices. AppA from *Rhodobacter sphaeroides* is a representative BLUF protein and functions as a transcriptional antirepressor of photosynthetic genes.[3] Figure 1 shows the X-ray structures of the BLUF domain of wild-type (WT) AppA[16] (panel A) and the Cys20→Ser (C20S) mutant[19] (panel B). FAD is involved in an extensive hydrogen-bond network with the side chains lining its binding pocket, including a highly conserved tyrosine (Tyr21), glutamine (Gln63), and tryptophan (Trp104). A light-induced rearrangement of the hydrogen-bond network is believed to result in the formation of a signaling state, and its structural information is essential to understand the photocycle mechanism of BLUF proteins. However, although the overall

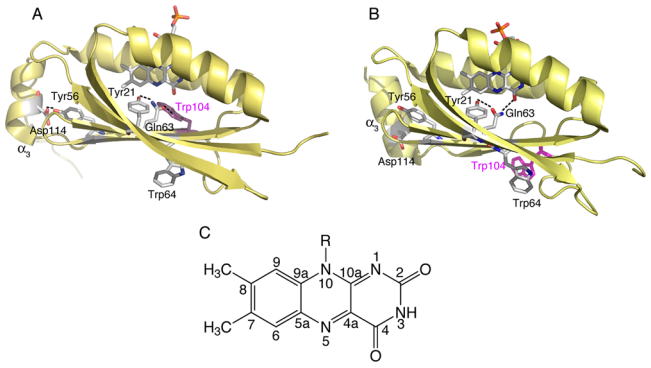

Figure 1. X-ray structures of the wild-type AppA133 (A) and the C20S mutant of AppA126 (B). The vicinity of the FAD chromophore and tryptophan and tyrosine residues are highlighted. The coordinates were taken from Protein Data bank ID (A) 1YRX[16] and (B) 2IYG.[19] Panel C shows the structure and numbering of the FAD isoalloxazine ring.

Received: June 14, 2012
Published: June 27, 2012

protein structure has been well established, there still exists a key ambiguity regarding the position and orientation of Gln63 and Trp104 with respect to the flavin moiety. As shown in Figure 1A, the crystal structure of the BLUF domain of WT AppA shows that Trp104, which is located in the $\beta4-\beta5$ loop, is found in the vicinity of FAD and forms a hydrogen bond with a side chain of Gln63.[16] We denote the structure as Trp_{in}, and this structure is supported by several spectroscopic,[24−27] NMR,[18,23] and computational studies.[28,29] On the other hand, the X-ray crystal structure of the C20S mutant revealed that it had the Trp_{out} conformation, in which Trp104 is exposed to the solvent and is located more than 10 Å from Gln63.[19] The latter Trp_{out} conformation has also been observed for several BLUF proteins, such as PixD from *T. elongates* BP-1 (Tll0078)[17] and BlrB from *Rhodobacter sphaeroides*.[8] Furthermore, the crystal structures of PixD from *Synechocystis* sp. PCC6803 (Slr1694) show the Trp_{out} conformation with the exception that one of ten crystallographic subunits adopts the Trp_{in} conformation.[20] The two opposing structures indicate the dynamic nature of the $\beta4-\beta5$ loop moiety, and several spectroscopic and theoretical studies[30−34] suggested that Trp104 undergoes light-dependent alterations in its chemical environment. In fact, in vivo and in vitro site-directed analyses of AppA[33] have demonstrated a crucial role of Trp104 to a light-dependent antirepressor activity of AppA. These spectroscopic and biochemical studies indicate that the $\beta4-\beta5$ region plays a critical role in blue-light sensing by BLUF domains.

Recently, however, Dragnea et al.[30] pointed out that the two published crystal structures of AppA BLUF domains have slightly different N- and C-termini. The Trp_{in} conformation[16] was obtained from an AppA BLUF domain composed of amino acids 17 through 133 (AppA133), whereas the Trp_{out} conformation[19] was obtained from the C20S mutant that extended from amino acids 1 through 124. In addition, a comparative study using AppA133 and AppA126, which is composed of amino acids 1 through 126, showed the influence of an N-terminal truncation on the conformation and/or environment of Trp104 and suggested that the Trp_{in} conformation is an artifact of the N-terminal truncation.[30] Because Trp104 is one of the key amino acid residues for the function of AppA,[34,35] it is essential to clarify whether the alteration of the amino acid sequences from AppA126 to AppA133 causes the protein conformational change from Trp_{out} to Trp_{in}. For this purpose, we compared the solution structures of AppA126 and AppA133 with respect to two points. First, as illustrated in Figure 1A, the Trp_{in} conformation has no hydrogen bond between the Gln63 side chain and the flavin C4═O group. In contrast, the amine group of Gln63 forms a hydrogen bond with the C4═O oxygen in Trp_{out} (Figure 1B). We therefore expect that the vibrational spectra of the flavin ring differ between AppA126 and AppA133. To examine this point, we have applied near-infrared Raman (NIRR) spectroscopy to measure the vibrational spectra of the flavin moiety. According to a previous study,[14,26] NIRR spectroscopy will be able to monitor the C4═O stretching mode around 1710 cm^{-1}, which is a sensitive guide for revealing the presence or absence of the hydrogen bond at the C4═O moiety. Another issue that we focus on in the present study is the location of Trp104. To compare the structures and environments of Trp104 between AppA126 and AppA133, we used ultraviolet resonance Raman (UVRR) spectroscopy. As we have shown previously, the resonance Raman measurements with 224.3 nm excitation result in strong enhancement of the vibrational modes for aromatic residues such as tryptophan and tyrosine, with a little interference from the chromophore and the remaining protein moiety.[27] Thus, the UVRR spectra of AppA126 and AppA133 can be used to directly compare the structures and environments of Trp104. As described below, the NIRR and UVRR data provide evidence of slight structural differences between AppA126 and AppA133, and the implications of these observations will be discussed.

EXPERIMENTAL PROCEDURES

Sample Preparations. AppA126 and AppA133 were expressed and purified as described previously.[13,16]

Near-Infrared Raman Spectroscopy. A diode laser (StarBright 785 XM; Torsana Laser Technologies, Sweden) was used to measure the Raman spectra. The laser beam was focused by a lens (F/15, f = 150 mm) into samples contained in a 3 × 3 × 48 mm quartz cuvette, and two 45° rod mirrors (Edmund Optics Inc.) were used to steer the laser light to the sample. The backscattered light from the sample was collected by an aspheric glass condenser lens (F/0.8, f = 20 mm) and refocused by an achromatic lens (F/1, f = 30 mm) to the end of a fiber bundle with a core diameter of 100 μm. A long-pass edge filter (OD > 6; Semrock Inc.) was used to reject the laser light before the refocusing lens. The light was directed into a spectrometer (Acton LS 785; Princeton Instruments) equipped with a thermoelectrically cooled CCD detector (PIXIS: 256E; Princeton Instruments). All spectra were taken at room temperature (~25 °C), and homemade software was used to eliminate the noise spikes in the spectra caused by cosmic rays. All Raman spectra were calibrated using neat fenchone.

Ultraviolet Resonance Raman Spectroscopy. UVRR spectroscopy was carried out with a hollow cathode HeAg Laser system as described previously.[27] A 224.3 nm light from the HeAg laser was used to measure the UVRR spectra, and the spectra were measured every 30 min to ensure little contribution of the signaling state formed by the probe light. The laser was operated to produce 0.3 μJ/pulse at the sample. All spectra were taken at room temperature (~25 °C) and were calibrated by using neat cyclohexane as a standard. Sample volumes were 150 μL and were contained in a quartz spinning cell (10 mm in diameter). The cell was spun at 1600 rpm. The Raman cross sections of the 932 cm^{-1} band of perchlorate determined by Dudik et al.[36] were used to calculate the Raman cross sections of tryptophan as described previously.[37]

RESULTS

During the purification process, we found that AppA133 tends to precipitate under a high protein concentration. Thus AppA133 was dissolved in a buffer containing 200 mM NaCl throughout this study. (We have confirmed that different salt concentrations did not affect the UV−vis absorption spectra nor the dark recovery kinetics of AppA126; see Figures S1 and S2 in Supporting Information.) Although AppA133 is somewhat unstable compared to AppA126, the two proteins show similar UV−vis absorption spectra with absorption maxima λ_{max} of 446 nm. A similar result was also reported previously.[30] Figure 2 compares the NIRR spectra of WT AppA126 (trace a) and AppA133 (trace b) under the dark state. The Raman spectra were obtained with a near-infrared (NIR) excitation (λ_{ex} = 785 nm) to avoid fluorescence from the samples. Most of the observed bands in the spectra can be assigned to vibrational modes for the FAD chromophore, and a shoulder at 1706 cm^{-1}

dx.doi.org/10.1021/jp305873z | J. Phys. Chem. B 2012, 116, 8974−8980

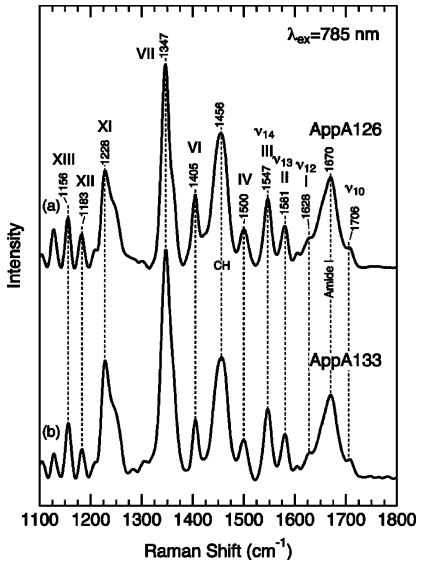

Figure 2. Near-infrared Raman spectra of wild-type AppA126 (a) and AppA133 (b). The buffer compositions were 5 mM Tris-HCl, 1 mM NaCl, pH 8.0 (AppA126), and 20 mM Tris-HCl, 200 mM NaCl, pH 8.0 (AppA133). The spectra were obtained at 785 nm excitation. The notation introduced by Bowman and Spiro[38] is designated in the figure.

on the broad amide I band around 1670 cm^{-1} is assigned to the carbonyl C4=O stretching vibration ν_{10} of the isoalloxazine ring.[14,26,39] The two spectra are very similar to each other, and there is no detectable difference in the ν_{10} frequency between AppA126 and AppA133. This result indicates that the state of hydrogen bonding at the C4=O position is largely the same, because the C=O stretching frequency is highly sensitive to the presence or absence of a hydrogen bond at the carbonyl oxygen.[14,26] In addition to ν_{10}, the two samples exhibit almost identical frequencies for the Raman bands of the flavin moiety, such as bands I, II, and III. These bands are assigned to ν_{12} (1628 cm^{-1}), ν_{13} (1581 cm^{-1}), and ν_{14} (1547 cm^{-1}), respectively, and mainly involve C=C stretching and/or C=N stretching vibrations of the isoalloxazine ring.[26,39] Because these vibrational modes are also expected to be sensitive to a hydrogen bond at the C4=O moiety, the similar frequencies for these bands further indicate that there are only slight structural differences between the active sites of AppA126 and AppA133. A similar hydrogen-bonding environment of the isoalloxazine ring is also consistent with an identical absorption maximum λ_{max}, because a previous DFT study showed that the presence or absence of a hydrogen bond at the C4=O or N5 position affects λ_{max} by ~10 nm.[14]

We next examined the structures and environments of Trp104 through UVRR spectroscopy. Previous UVRR studies have shown that the Raman intensities of tryptophan residues depend sensitively on the polarity of the solvent environment.[40−42] For instance, Chi and Asher[41] observed that in water−propanol solvent mixtures the Raman cross sections of tryptophan with 229 nm excitation increase with decreasing water composition. Because the observed increase in intensity was ascribed to red shifts of the ~220 nm tryptophan absorption band, an increase or decrease in the Raman intensities will depend on the excitation wavelength. To establish the relationship between the Raman intensities with 224.3 nm excitation and environmental polarity, we measured the UVRR spectra of tryptophan in water−propanol solvent mixtures, and the results are shown in Figure 3. The UVRR spectra of tryptophan mainly consist of bands at 761, 1011,

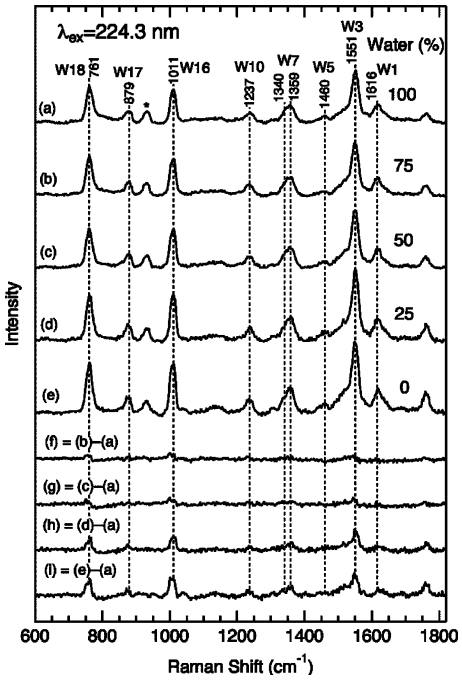

Figure 3. UVRR spectra of tryptophan with 224.3 nm excitation in different water−propanol solvent mixtures. The Raman spectra of the solvent mixtures are subtracted. The concentrations of tryptophan and $NaClO_4$ were 0.3 mM and 0.74 M, respectively. The asterisk indicates a Raman band of ClO_4^-.

1551, and 1616 cm^{-1}, and these are assigned to W18 (the indole ring-breathing), W16 (benzene ring-breathing), W3 (C−C stretching of the pyrrole ring), and W1 (C=C stretching of the benzene ring), respectively.[43] The 933 cm^{-1} band derives from the internal standard perchlorate stretching, and bands from water−propanol mixtures are subtracted from the spectra. The frequencies and band shapes of the tryptophan bands remain relatively constant, while the intensities increase as the solvent changes from pure water to pure propanol (traces a→e). Figure 4, which plots the Raman cross sections for W3,

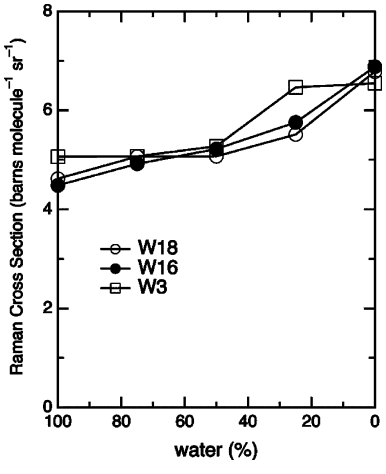

Figure 4. Solvent composition-dependence of the Raman cross sections of tryptophan at 224.3 nm excitation.

dx.doi.org/10.1021/jp305873z | J. Phys. Chem. B 2012, 116, 8974−8980

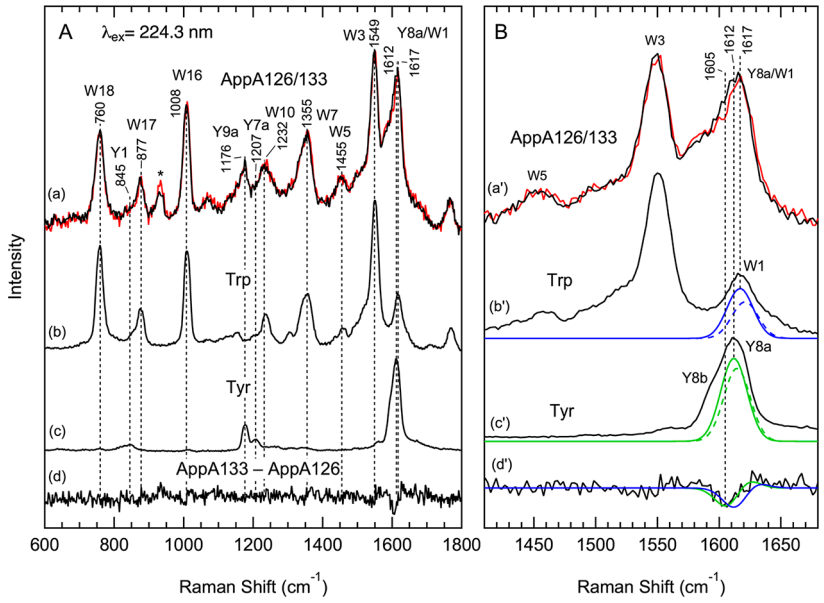

Figure 5. UVRR spectra of AppA126 (black) and AppA133 (red) (a, a′), tryptophan (b, b′), and tyrosine (c, c′), and the AppA133 minus AppA126 difference spectrum (d, d′). The spectra were obtained at 224.3 nm excitation. Panel B is an expanded plot of the high frequency region. The blue and green traces in panel B are simulated Raman bands of the W1 and Y8a modes and their difference spectra, respectively. The details are given in the text. The protein concentrations were ca. 50 μM, and the buffer compositions were 5 mM Tris-HCl, 1 mM NaCl, pH 8.0, 0.1 M NaClO (AppA126) and 20 mM Tris-HCl, 200 mM NaCl, pH 8.0, 0.1 M NaClO (AppA133).

W16, and W18 as a function of water concentration, shows that the Raman cross sections monotonically increase as the water concentration decreases. These observations indicate that, in analogy with the case of the 229 nm excitation,[41] the Raman cross sections of tryptophan with 224.3 nm excitation increase as the environmental polarity decreases. This agrees with a previous result that the Raman cross section of the W3 band for tryptophan in 70% ethylene glycol is larger than that for tryptophan in aqueous solution.[40]

Now we know that the Raman intensities are a good measure of the polar environment of the tryptophan residue. Next we compared the UVRR spectra of AppA126 and AppA133 in Figure 5A (traces a). The spectra are normalized by considering the heights of the perchlorate bands at 932 cm^{-1} and the sample concentrations. The spectra for aqueous solutions of tryptophan (trace b) and tyrosine (trace c) are also illustrated in the figure. These data indicate that the UVRR spectra for AppA126 and AppA133 contain several Raman bands that mainly arise from tryptophan (trace b) and tyrosine residues (trace c). As seen in the figure, tryptophan bands W18, W16, and W3 dominate the UVRR spectra of the BLUF domains of AppA. Because both AppA126 and AppA133 contain two tryptophan residues, i.e., Trp64 and Trp104, both of these residues contribute to the observed Raman bands. The main Raman band of tyrosine is observed at 1617 cm^{-1} and is assigned to the ring C−C stretching mode Y8a.[43] Although this Raman band overlaps with the W1 band of tryptophan, the ratio of the intensity of the W1 band to the W3 band of tryptophan in an aqueous solution (trace b) indicate that Y8a is a dominant contributor to the band at 1616 cm^{-1}.

A comparison of the UVRR spectra between AppA126 (the black line in trace a) and AppA133 (the red line in trace a) in Figure 5A demonstrates that their spectra are similar to each other. A lack of major spectral differences is clearly illustrated in the AppA133 − AppA126 difference spectrum (trace d). In particular, there is very little difference among the intensities of the W18, W16, and W3 bands. Although no detectable intensity difference is seen for these bands, we observed a negative feature at around 1605 cm^{-1} in the difference spectrum. Because a main contributor to the band around 1615 cm^{-1} is Y8a for tyrosine, it is likely that the structures and/or environments of tyrosine residues differ between AppA126 and AppA133. To examine the contribution of Y8a to the feature around 1605 cm^{-1}, we performed the simple spectral simulations presented in Figure 5B, which show the high frequency region of the UVRR spectra as well as the simulated spectra. When Gaussian bands (bandwidth 25 cm^{-1}) with different intensities were assumed at 1612 and 1614.5 cm^{-1}, as shown by the green lines in trace c′, their difference spectrum well reproduced the observed spectrum (trace d′). This implies that the 1605 cm^{-1} feature can be ascribed to a band shift as well as an intensity change of Y8a. Note that although the W1 band overlaps with Y8a, its frequency is higher than that of Y8a (see Figure 5B). In our previous study[27] we measured the UVRR spectra of Trp64→Phe (W64F) and Trp104→Ala (W104A) mutants and estimated that the W1 frequency for Trp64 and Trp104 is about 1620 cm^{-1}. As shown by the blue lines in Figure 5B, the W1 frequency is too high to reproduce the difference feature (the blue lines in Figure 5B represent simulated Raman bands at 1617 and 1621 cm^{-1} and their difference spectrum), suggesting that the spectral change near 1605 cm^{-1} is due to the Y8a band of tyrosine.

■ DISCUSSION

Using NIRR spectroscopy, we found that both AppA126 and AppA133 contain a similar hydrogen-bonding network around the flavin ring (Figure 2). The structure and environment of tryptophan residues are also indistinguishable between the two BLUF constructs (Figure 5). These observations rule out the previous proposal that the N-terminal truncation in AppA133 leads to the Trp_{in} conformation, whereas the N-terminal intact AppA126 shows the Trp_{out} conformation.[30] These authors

dx.doi.org/10.1021/jp305873z | J. Phys. Chem. B 2012, 116, 8974−8980

compared AppA126 and AppA133 using a combination of NMR, fluorescence, and acrylamide quenching of tryptophan fluorescence, and their proposal was based on some spectroscopic differences between AppA126 and AppA133. It is, however, likely that the observed spectroscopic distinctions reflect minor structural differences. In fact, although the fluorescence maxima from tryptophan residues are slightly different between WT AppA126 (336 nm) and AppA133 (333 nm), the corresponding W64F mutants, in which only Trp104 exists, exhibit a similar fluorescence maximum (~330 nm) that is typical for a buried environment. Analogously, while a distinct difference was observed for the fluorescence quenching experiments for WT proteins, a minor difference was observed for the W64F mutants. For example, the fluorescence quenching by acrylamide differs by at most ~20% between the W64F mutants of AppA126 and AppA133. Here we should note that the first systematic study on tryptophan fluorescence in the AppA BLUF domain (residues 5−125) and its W64F mutant was carried out by Toh et al.,[25] who arrived at a similar conclusion regarding the buried conformation of Trp104 in the dark as well as in the signaling states.

As discussed above, the results presented here show that the N-terminal truncation does not induce a conformational switch between Trp_{in} and Trp_{out}. There is, however, no evidence showing which conformation is realized in solution. In a previous UVRR study on AppA126, we observed that the Gln63→Leu (Q63L) mutation significantly reduced the intensities of tryptophan Raman bands.[27] As shown in Figures 3 and 4, the 224.3 nm excited Raman cross sections for tryptophan decrease with increasing water composition. The reduced intensities of tryptophan Raman bands are consistent with the idea that the Q63L mutation alters the Trp_{in} conformation of WT AppA126 to Trp_{out}. This implies that WT AppA126 as well as AppA133 adopt the Trp_{in} conformation in solution.

Here we should discuss a structural difference between AppA126 and AppA133. As described above, the present study demonstrates a lack of effect of the N-terminal truncation on the Trp_{in}/Trp_{out} conformational change, but we observed a spectral difference at 1605 cm^{-1} for the Y8a band of tyrosine. The BLUF domain of AppA contains two tyrosine residues at positions 21 and 56. Tyr21 is located in the vicinity of the isoalloxazine ring and forms a hydrogen bond with the side chain of Gln63 (Figure 1). Because the Raman spectra of the isoalloxazine ring are indistinguishable between AppA126 and AppA133 (Figure 2), the hydrogen-bonding network at the active site should be largely the same. It is therefore likely that the spectral difference near 1605 cm^{-1} is due to the remaining tyrosine residue Tyr56. To confirm the spectral change of Tyr56, we constructed Y56F/W64F double mutants for AppA126 and AppA133. The AppA126 mutant binds FAD normally, but the flavin chromophore was easily lost during the purification process for the AppA133 mutant. This prevented us from confirming the origin of the 1605 cm^{-1} feature, but the structures and/or environments of Tyr56 probably differ between AppA126 and AppA133. As depicted in Figure 1, Tyr56 is positioned far from the flavin and faces the α_3 helix in the crystal structures.[16,19] In contrast to the core of the BLUF domain, the C-terminal α_3 helix seems to be dynamic in nature. The two crystal structures of the AppA BLUF domains show a clear difference in the relative positions of the α_3 helix, e.g., Tyr56 forms a hydrogen bond with Asp114 in the WT crystal structure,[16] whereas this hydrogen bond is broken in the structure of the C20S mutant.[19] The dynamic nature of the C terminal extension was also shown for the BLUF domain of BlrB from *Rhodobacter sphaeroides*.[22] Thus it is possible that a different C-terminal extension affects the location of the α_3 helix, leading to an environmental difference in Tyr56. Here we note that previous ultrafast time-resolved infrared spectroscopy on PixD[44,45] observed an infrared band around 1620 cm^{-1}, and this band was also assigned to Y8a of tyrosine. However, this infrared feature detected at an early stage of the photocycle was ascribed to Tyr8 (Tyr21 in AppA), which is located in the active site.

Finally, we discuss the implication of the present results for the photocycle mechanism of the BLUF proteins. Previous crystallographic studies of BLUF domains[16,19,20] suggested that Trp104 plays a central role in the formation of a signaling state. The importance of Trp104 was also supported by a biochemical and genetic study showing that the W104A mutant is functionally locked in the signaling state.[34] A photocycle mechanism proposed by Anderson et al.[16] considers the Trp_{in} conformation as a dark state (Figure 1A), and it is assumed that the signaling state is reached by a ~180° rotation of the Gln63 side chain resulting in a new hydrogen bond between the amino group of the Gln63 side chain and the flavin O4. Yuan et al.[20] further suggested that the flip of the side chain of Gln63 accompanies a movement of Trp104 from Trp_{in} to Trp_{out} conformation. On the other hand, Jung et al.[19] reported the Trp_{out} structure for the C20S mutant of AppA BLUF domain. Their photocycle model involves the light-induced conformational change from Trp_{out} to Trp_{in}. This discrepancy has led to some theoretical studies on the photocycle and the conformation of the AppA BLUF domain in the dark and signaling states. Obanayama et al.[33] performed molecular dynamics calculations as well as quantum chemical calculations. They suggested that the light-induced structural change is associated with the Trp104 movement from the Trp_{out} to Trp_{in} conformation without a flip of Gln63 side chain. Domratcheva et al.[32] applied a combined quantum mechanical and molecular mechanical (QM/MM) method to BLUF domains and assigned the Trp_{out} conformation to the dark state. In their model, light activation results in the Trp_{in} conformation with a 180° rotation of the Gln63 side chain followed by tautomerization of the Gln63 side chain to its imidic form. From a QM/MM study, Sadeghian et al.[31] also reached to a similar photocycle model involving the tautomerization, but the rotation of the Gln63 side chain is excluded from their model. Their photocycle model also involves a change from the Trp_{out} to the Trp_{in} conformation. Although the present study does not provide direct information concerning the structure of the light-induced signaling state, the photocycle model that considers Trp_{in} as a dark state[16,20] appears to be consistent with our findings. As we showed previously,[27] however, the formation of a signaling state does not accompany a large intensity change in the UVRR spectrum of Trp104. This observation suggests that Trp104 would be buried in both the dark and signaling states. A similar conclusion was also suggested by a tryptophan fluorescence study by Toh et al.[25]

In conclusion, the effect of the N-terminal truncation was examined by comparing AppA126 and AppA133 through NIRR and UVRR spectroscopy. The NIRR data indicate that there is no detectable difference in the vibrational frequencies of the isoalloxazine ring. This observation strongly suggests that the hydrogen-bonding network at the active site is indistinguishable between the two BLUF constructs. The UVRR spectra were

also measured to compare the structures and environments of the Trp104 residue. Because the intensities of the tryptophan Raman bands are essentially the same, we conclude that the N-terminal truncation in AppA133 does not induce the conformational change between Trp_{in} and Trp_{out}. These observations along with the previous UVRR data for the Q63L mutant[27] suggest that the Trp_{in} conformation applies for both AppA126 and AppA133 under the dark state. This result resolves a controversy concerning the location of Trp104. We should keep in mind, however, that the above conclusion contradicts the crystal structures of Tll0077,[7] BlrB,[8] and nine of ten crystallographic subunits of Slr1694,[20] where Trp_{out} conformations have been reported. Thus, the location of the tryptophan residue may differ between AppA and other BLUF proteins, as suggested previously.[46] In addition, a part of the results for the BLUF domains of AppA might not be applicable to a full-length protein. These issues remain for a future study.

■ ASSOCIATED CONTENT

Supporting Information

Supplemental data. This material is available free of charge via the Internet at http://pubs.acs.org.

■ AUTHOR INFORMATION

Corresponding Author

*E-mail: unno@cc.saga-u.ac.jp.

Notes

The authors declare no competing financial interest.

■ ACKNOWLEDGMENTS

This study was supported by KAKENHI (23550019 to M.U.) and the Mistubishi Foundation (M.U.).

■ REFERENCES

(1) van der Horst, M. A.; Hellingwerf, K. J. *Acc. Chem. Res.* **2004**, *37*, 13−20.
(2) Gomelsky, M.; Klug, G. *Trends Biochem. Sci.* **2005**, *27*, 497−500.
(3) Masuda, S.; Bauer, C. E. In *Handbook of Photosensory Receptors*; Briggs, W. R.; Spudich, J., Eds.; Wiley-VCH Verlag GmbH: Weinheim. 2005; pp 433−445.
(4) Zoltowski, B. D.; Gardner, K. H. *Biochemistry* **2011**, *50*, 4−16.
(5) Masuda, S.; Bauer, C. E. *Cell* **2002**, *110*, 613−623.
(6) Kraft, B. J.; Masuda, S.; Kikuchi, J.; Dragnea, V.; Tollin, G.; Zaleski, J. M.; Bauer, C. E. *Biochemistry* **2003**, *42*, 6726−6734.
(7) Masuda, S.; Hasegawa, K.; Ishii, A.; Ono, T. *Biochemistry* **2004**, *43*, 5304−5313.
(8) Jung, A.; Domratcheva, T.; Tarutina, M; Wu, Q.; Ko, W.-H.; Shoeman, R. L.; Gomelsky, M.; Gardner, K. H.; Schlichting, I. *Proc. Natl. Acad. Sci. U.S.A.* **2005**, *102*, 12350−12355.
(9) Rajagopal, S.; Key, J. M.; Purcell, E. B.; Boerema, D. J.; Moffat, K. *Photochem. Photobiol.* **2005**, *80*, 542−547.
(10) Fukushima, Y.; Okajima, K.; Shibata, Y.; Ikeuchi, M.; Itoh, S. *Biochemistry* **2005**, *44*, 5149−5158.
(11) Gauden, M.; Yeremenko, S.; Laan, W.; van Stokkum, I. H. M.; Ihalainen, J. A.; van Grondelle, R.; Hellingwerf, K. J.; Kennis, J. T. M. *Biochemistry* **2005**, *44*, 3653−3662.
(12) Ito, S.; Murakami, A.; Sato, K.; Nishina, Y.; Shiga, K.; Takahashi, T.; Higashi, S.; Iseki, M.; Watanabe, K. *Photochem. Photobiol. Sci.* **2005**, *4*, 762−769.
(13) Masuda, S.; Hasegawa, K.; Ono, T. *Biochemistry* **2005**, *44*, 1215−1224.
(14) Unno, M.; Sano, R.; Masuda, S.; Ono, T.; Yamauchi, S. *J. Phys. Chem. B* **2005**, *109*, 12620−12626.
(15) Okajima, K.; Fukushima, Y.; Suzuki, H.; Kita, A.; Ochiai, Y.; Katayama, M.; Shibata, Y.; Miki, K.; Noguchi, T.; Itoh, S.; Ikeuchi, M. *J. Mol. Biol.* **2006**, *363*, 10−18.
(16) Anderson, S.; Dragnea, V.; Masuda, S.; Ybe, J.; Moffat, K.; Bauer, C. *Biochemistry* **2005**, *44*, 7998−8005.
(17) Kita, A.; Okajima, K.; Morimoto, Y.; Ikeuchi, M.; Miki, K. *J. Mol. Biol.* **2005**, *349*, 1−9.
(18) Grinstead, J. S.; Hsu, S.-T. D.; Laan, W.; Bonvin, A. M. J. J.; Hellingwerf, K. J.; Boelens, R.; Kaptein, R. *ChemBioChem* **2006**, *7*, 187−193.
(19) Jung, A.; Reinstein, J.; Domratcheva, T.; Shoeman, R. L.; Schlichting, I. *J. Mol. Biol.* **2006**, *362*, 717−732.
(20) Yuan, H.; Anderson, S.; Masuda, S.; Dragnea, V.; Moffat, K.; Bauer, C. *Biochemistry* **2006**, *45*, 12687−12694.
(21) Wu, Q.; Gardner, K. H. *Biochemistry* **2009**, *48*, 2620−2629.
(22) Barends, T. R. M.; Hartmann, E.; Griese, J. J.; Beitlich, T.; Kirienko, N. V.; Ryjenkov, D. A.; Reinstein, J.; Shoeman, R. L.; Gomelsky, M.; Schlichting, I. *Nature* **2009**, *459*, 1015−1018.
(23) Grinstead, J.; Avila-Perez, M; Hellingwerf, K.; Boelens, R.; Kaptein, R. *J. Am. Chem. Soc.* **2006**, *128*, 15066−15067.
(24) Gauden, M.; Grinstead, J. S.; Laan, W.; van Stokkum, I. H. M.; Avila-Perez, M.; Toh, K. C.; Boelens, R.; Kaptein, R.; van Grondelle, R.; Hellingwerf, K. J.; Kennis, J. T. M. *Biochemistry* **2007**, *46*, 7405−7415.
(25) Toh, K. C.; van Stokkum, I. H.; Hendriks, J. C.; Alexandre, M. T.; Arents, J. C.; Avila-Perez, M.; van Grondelle, R.; Hellingwerf, K. J.; Kennis, J. T. M. *Biophys. J.* **2008**, *95*, 312−321.
(26) Unno, M.; Masuda, S.; Ono, T.; Yamauchi, S. *J. Am. Chem. Soc.* **2006**, *128*, 5638−5639.
(27) Unno, M.; Kikuchi, S.; Masuda, S. *Biophys. J.* **2010**, *98*, 1949−1956.
(28) Meier, K.; Thiel, W.; van Gunsteren, W. F. *J. Comput. Chem.* **2012**, *33*, 363−378.
(29) Rieff, B.; Bauer, S.; Mathias, G.; Tavan, P. *J. Phys. Chem. B* **2011**, *115*, 11239−11253.
(30) Dragnea, V.; Arunkumar, A. I.; Yuan, H.; Giedroc, D. P.; Bauer, C. E. *Biochemistry* **2009**, *48*, 9969−9979.
(31) Sadeghian, K.; Bocola, M.; Schutz, M. *J. Am. Chem. Soc.* **2008**, *130*, 12501−12513.
(32) Domratcheva, T.; Grigorenko, B. L.; Schlichting, I.; Nemukhin, A. V. *Biophys. J.* **2008**, *94*, 3872−3879.
(33) Obanayama, K.; Kobayashi, H.; Fukushima, K.; Sakurai, M. *Photochem. Photobiol.* **2008**, *84*, 1003−1010.
(34) Masuda, S.; Tomida, Y.; Ohta, H.; Takamiya, K. *J. Mol. Biol.* **2007**, *368*, 1223−1230.
(35) Masuda, S.; Hasegawa, K.; Ono, T. *Plant Cell Physiol.* **2005**, *46*, 1894−1901.
(36) Dudik, J. M.; Johnson, C. K.; Asher, S. A. *J. Chem. Phys.* **1985**, *82*, 1732−1740.
(37) El-Mashtoly, S. F.; Yamauchi, S.; Kumauchi, M.; Hamada, N.; Tokunaga, F.; Unno, M. *J. Phys. Chem. B* **2005**, *109*, 23666−23673.
(38) Bowman, W. D.; Spiro, T. G. *Biochemistry* **1981**, *20*, 3313−3318.
(39) Kikuchi, S.; Unno, M.; Zikihara, K.; Tokutomi, S.; Yamauchi, S. *J. Phys. Chem. B* **2009**, *113*, 2913−2921.
(40) Rodger, K. R.; Su, C.; Subramaniam, S.; Spiro, T. G. *J. Am. Chem. Soc.* **1992**, *114*, 3697−3709.
(41) Chi, Z.; Asher, S. A. *J. Phys. Chem. B* **1998**, *102*, 9595−9602.
(42) Matsuno, M.; Takeuchi, H. *Bull. Chem. Soc. Jpn.* **1998**, *71*, 851−857.
(43) Harada, I.; Takeuchi, H. In *Spectroscopy of Biological Systems, Advances in Spectroscopy*; Clark, R. J. H., Hester, R. E., Eds.; John Wiley & Sons: Chichester, U.K., 1986; Vol. *13*, pp 113−175.
(44) Bonetti, C.; Mathes, T.; van Stokkum, I. H. M.; Mullen, K. M.; Groot, M.-L.; van Grondelle, R.; Hegemann, P.; Kennis, J. T. M. *Biophys. J.* **2008**, *95*, 4790−4802.
(45) Mathes, T.; Zhu, J.; van Stokkum, I. H. M.; Groot, M.-L.; Hegemann, P.; Kennis, J. T. M. *J. Phys. Chem. Lett.* **2011**, *3*, 203−208.

(46) Masuda, S.; Hasegawa, K.; Ohta, H.; Ono, T. *Plant Cell Physiol.* **2008**, *49*, 1600−1606.